GASLESS COMBUSTION FRONTS WITH HEAT LOSS

ANNA GHAZARYAN, STEPHEN SCHECTER, AND PETER L. SIMON

ABSTRACT. For a model of gasless combustion with heat loss, we use geometric singular perturbation theory to show existence of traveling combustion fronts. We show that the Evans function has a simple zero at the origin, and we show that if there are no other zeroes of the Evans function in $\mathrm{Re}\,\lambda \geq 0$, then the front is nonlinearly stable in an appropriate sense. For the case of a solid reactant, by numerically computing the Evans function on a large half circle, we give evidence that the Evans function condition is satisfied for some parameter values.

1. Introduction

We consider the "gasless combustion" model

$$\partial_t u_1 = \partial_{xx} u_1 + u_2 \rho(u_1 - \bar{u}_1) - \delta u_1, \tag{1.1}$$

$$\partial_t u_2 = \kappa \partial_{xx} u_2 - \beta u_2 \rho(u_1 - \bar{u}_1), \tag{1.2}$$

with $\beta > 0$, $\delta \geq 0$, $\kappa \geq 0$, and

$$\rho(u) = \begin{cases} e^{-\frac{1}{u}} & \text{if } u > 0, \\ 0 & \text{if } u \leq 0. \end{cases} \tag{1.3}$$

Here u_1 is temperature, u_2 is reactant concentration, $u_1 = \bar{u}_1$ is the temperature below which the reaction does not occur (ignition temperature), and $u_1 = 0$ is the ambient temperature. We assume that $\bar{u}_1 \geq 0$, so the reaction does not occur at the ambient temperature. ρ is the unit reaction rate, which is a function of temperature, and β is the "exothermicity" parameter; the larger β is, the more fuel one must burn to achieve a given increase in temperature. κ is the inverse of the Lewis number; if $\kappa = 0$, the reactant is a solid. The term δu_1 represents heat loss from the system to the environment according to Newton's law of cooling. The 4-tuple $(\beta, \bar{u}_1, \delta, \kappa)$ is a vector of parameters.

If we replace $u_2\rho(u_1)$ by a more general function $\omega(u_1, u_2)$, then, except in Section 5.2 where we do some numerics, the only properties of ω that are actually used are: ω is defined and C^3 on $\{(u_1, u_2) : -\beta^{-1} < u_1 \leq \beta^{-1}$ and $0 \leq u_2 \leq 1\}$; $\omega(u_1, u_2) = 0$ for $u_1 \leq 0$; $\omega > 0$ for $u_1 > 0$ and $u_2 > 0$; $\omega(u_1, 0) = 0$ for all u_1; and $\frac{\partial \omega}{\partial u_2}(\beta^{-1}, 0) > 0$.

Our interest is in traveling combustion fronts for the gasless combustion model and their stability. If such fronts travel to the right, they connect an unburned state at the right to a burned state at the left. By an unburned state we mean that the temperature u_1 is 0, the ambient temperature, and the reactant concentration u_2 is positive; we will normalize it to 1. If there is no heat loss to the environment (i.e., if $\delta = 0$), the burned state has a positive

Date: July 5, 2011.

1991 *Mathematics Subject Classification.* 80A25, 35K57, 35B40, 34E15.

Key words and phrases. geometric singular perturbation theory, traveling wave, Evans function, stability.

This work was supported in part by the National Science Foundation under grants DMS-0908009 and DMS-0708386, and by OTKA under grant 81403.

temperature (it turns out to be β^{-1}) and reactant concentration 0. If there is heat loss to the environment (i.e., if $\delta > 0$), the burned state has the ambient temperature $u_1 = 0$ and a positive reactant concentration; some of the reactant remains unburned. We shall always limit our attention to fronts that approach their end states exponentially.

Existence and stability of traveling waves for the gasless combustion model have been much studied. In Section 2 we review the literature, which often concerns various equivalent forms of the model.

In this paper we do several things that add to the known facts about the gasless combustion model.

1. In Section 3, we use geometric perturbation theory to show how combustion fronts for $\delta = 0$ perturb to combustion fronts for $\delta > 0$. Our result states that there exist continuous positive functions $\kappa_0(\beta, \bar{u}_1)$ and $\delta_0(\beta, \bar{u}_1)$, defined for $0 \le \bar{u}_1 < \beta^{-1}$, such that for $0 \le \kappa < \kappa_0(\beta, \bar{u}_1)$ and $0 \le \delta < \delta_0(\beta, \bar{u}_1)$, there is a unique wave speed $\sigma(\beta, \bar{u}_1, \delta, \kappa)$ near $\sigma(\beta, \bar{u}_1)$ defined above, with $\sigma(\beta, \bar{u}_1, 0, 0) = \sigma(\beta, \bar{u}_1)$, such that the system (1.1)–(1.2), with $\sigma = \sigma(\beta, \bar{u}_1, \delta, \kappa)$, has a traveling wave solution with the correct boundary behavior. The function $\sigma(\beta, \bar{u}_1, \delta, \kappa)$ is smooth.

2. In Section 4, we prove, for $\delta > 0$, that the traveling wave, if it is exists, is nonlinearly stable in an appropriate sense, provided the Evans function has no zeros in $\operatorname{Re} \lambda \ge 0$ other than a simple zero at the origin. The stability proof is nonstandard due to the fact that the essential spectrum of the linearized operator at the traveling wave touches the imaginary axis; when $\kappa = 0$ there is the additional difficulty that the essential spectrum includes a vertical line, so the operator is not sectorial. Machinery appropriate to dealing with these issues in a class of chemical reaction models that includes the gasless combustion model was developed in [9] and [10], generalizing the methods of [8] (for gasless combustion with $\delta = 0$ and $\kappa = 0$) and [6] (for gasless combustion with $\delta = 0$ and $\kappa > 0$).

More precisely, let $\mathcal{E}_0$ denote either $H^1(\mathbb{R})$ or BUC, the space of bounded uniformly continuous functions on $\mathbb{R}$ with the sup norm, and let $\mathcal{E}_\alpha$ denote the corresponding space with weight function $e^{\alpha\xi}$, $\xi = x - \sigma t$, where σ is the velocity of the combustion front; α is positive and small. Functions in $\mathcal{E}_\alpha$ decay exponentially as $\xi \to \infty$ but may grow exponentially as $\xi \to -\infty$; functions in $\mathcal{E}_0 \cap \mathcal{E}_\alpha$ decay exponentially as $\xi \to \infty$ and are bounded at the left. We show that perturbations of the combustion front that are small in $\mathcal{E}_0 \cap \mathcal{E}_\alpha$ decay exponentially in time to a shift of the combustion front in $\mathcal{E}_\alpha$. In addition, the u_1-component of the perturbation (temperature) decays exponentially in $\mathcal{E}_0$, and the u_2-component of the perturbation (reactant concentration) stays small in $\mathcal{E}_0$. Moreover, if $\kappa > 0$ and the perturbation is, in addition, in L^1, the u_2-component of the perturbation decays like $t^{-\frac{1}{2}}$ in the sup norm.

These results have the following interpretation. If the combustion front is perturbed in $\mathcal{E}_0 \cap \mathcal{E}_\alpha$, the solution looks like the combustion front at the right but not necessarily at the left. The temperature component of the perturbation rapidly decays in time; at the left this is because of heat loss to the environment. The reactant component of the perturbation may not decay in time at the left when $\kappa = 0$; this is because at the left, the temperature is too low for it to burn. (Both components of the perturbation decay exponentially at the right in time in the weighted norm, because initially they decay exponentially in space at the right, and, relative to the front, they move left.) On the other hand, when $\kappa > 0$ and the perturbation is, in addition, in L^1, the reactant component of the perturbation at the left does at least decay by diffusion as expected.

The behavior of temperature and reactant concentration is the reverse of their behavior when there is no heat loss to the environment; compare [8] and [6]. Without heat loss to the environment, the temperature behind the combustion front is high, so perturbations in the reactant concentration quickly decay (because the reactant burns), while perturbations in the temperature at best decay by diffusion.

3. In Section 5, we show analytically, for $\delta > 0$, that the Evans function for the combustion front of Section 3 has a simple zero at the origin. A similar result was obtained for $\delta = 0$ in [8] and [7]. As in those papers, the result is a consequence of the nondegenerate splitting of invariant manifolds that occurs in the construction of the front.

4. Also in Section 5, for $\kappa = 0$, β not too large, and $\delta > 0$, we provide numerical evidence that the Evans function for the combustion front of Section 3 has no zeros in $\operatorname{Re}\lambda \geq 0$, other than the simple zero at the origin. Similar numerical results have previously been obtained for the other cases; see the following section.

2. Literature on the gasless combustion model

Instead of the combustion model (1.1)–(1.2), several equivalent forms are often used in the literature.

One equivalent form is

$$\partial_t u_1 = \partial_{xx} u_1 + u_2 \hat{\rho}(u_1 - \bar{u}_1) - \delta u_1, \tag{2.1}$$

$$\partial_t u_2 = \kappa \partial_{xx} u_2 - u_2 \hat{\rho}(u_1 - \bar{u}_1), \tag{2.2}$$

where $\hat{\rho}$ is a function chosen from a one-parameter family of functions with properties similar to those of ρ, $\bar{u}_1 \geq 0$, $\delta \geq 0$, and $\kappa \geq 0$. To derive (2.1)–(2.2) from (1.1)–(1.2), in (1.1)–(1.2) make the substitution $u_1 = \frac{1}{\beta}\tilde{u}_1$. After dropping the tildes, one obtains (2.1)–(2.2) with $\hat{\rho}(u) = \beta\rho\left(\frac{u}{\beta}\right)$.

Another equivalent form is

$$\partial_t u_1 = \partial_{xx} u_1 + u_2 \epsilon^{-2} e^{\frac{1}{\epsilon}} \rho(\epsilon(u_1 - \bar{u}_1)) - \hat{\delta} u, \tag{2.3}$$

$$\partial_t u_2 = \kappa \partial_{xx} u_2 - u_2 \epsilon^{-2} e^{\frac{1}{\epsilon}} \rho(\epsilon(u_1 - \bar{u}_1)), \tag{2.4}$$

with $\epsilon > 0$, $\bar{u}_1 \geq 0$, $\hat{\delta} \geq 0$, and $\kappa \geq 0$. Studying the limit $\epsilon \to 0$ is called "high activation energy asymptotics." To derive (2.3)–(2.4) from (1.1)–(1.2), in (1.1)–(1.2) make the substitutions

$$\beta = \epsilon^{-1}, \quad u_1 = \epsilon \tilde{u}_1, \quad u_2 = \tilde{u}_2, \quad t = \epsilon^{-1} e^{\frac{1}{\epsilon}} \tilde{t}, \quad x = \left(\epsilon^{-1} e^{\frac{1}{\epsilon}}\right)^{\frac{1}{2}} \tilde{x}.$$

After dropping the tildes, one obtains (2.3)–(2.4) with $\hat{\delta} = \epsilon^{-1} e^{\frac{1}{\epsilon}} \delta$.

Remark 2.1. An alternative to (1.1)–(1.2) that is not equivalent to it is the system

$$\partial_t u_1 = \partial_{xx} u_1 + u_2 \rho(u_1) - \delta(u_1 - u_1^\dagger), \tag{2.5}$$

$$\partial_t u_2 = \kappa \partial_{xx} u_2 - \beta u_2 \rho(u_1). \tag{2.6}$$

In this system, which is better physically motivated than (1.1)–(1.2), $u_1 = 0$ is absolute zero, and $u_1^\dagger \geq 0$ is ambient temperature. Unfortunately, if $u_1^\dagger > 0$, physically meaningful traveling waves do not exist. This is called the "cold boundary difficulty": the boundary is not cold enough. Nevertheless, approximate traveling waves have been studied numerically [12].

The system (2.5)–(2.6) is sometimes altered by replacing the Arrhenius reaction rate function $\rho(u_1)$ by the discontinuous function

$$\rho_{\bar{u}_1}(u) = \begin{cases} e^{-\frac{1}{u}} & \text{if } u \geq \bar{u}_1, \\ 0 & \text{if } u < \bar{u}_1, \end{cases} \tag{2.7}$$

where $\bar{u}_1 > 0$ is ignition temperature. If $0 \leq u_1^\dagger \leq \bar{u}_1$, physically meaningful traveling waves often exist [1].

We shall now briefly review the literature on existence and stability of traveling combustion fronts for (1.1)–(1.2). We limit our discussion to fronts that approach their end states exponentially; this is only a limitation when $\bar{u}_1 = 0$, i.e., ignition temperature and ambient temperature are equal. Without loss of generality we restrict our attention to waves with positive velocity.

2.1. **Literature on traveling combustion fronts for (1.1)–(1.2) with no heat loss ($\delta = 0$).** We consider fronts with values $(u_1, u_2) = (u_1^*, 0)$ at the left and $(u_1, u_2) = (0, 1)$ at the right, where u_1^* is the temperature of combustion. It must be determined; it turns out to be β^{-1}. We therefore assume $\bar{u}_1 < \beta^{-1}$, i.e., ignition temperature is less than the temperature of combustion.

2.1.1. *Existence and uniqueness.* For infinite Lewis number ($\kappa = 0$) and $\bar{u}_1 = 0$, existence of a traveling front is shown in [4, 21]: the system reduces to one second-order equation by means of a first integral, and the proof is by phase plane analysis. The same proof would work for $0 < \bar{u}_1 < \beta^{-1}$. Uniqueness follows from the Melnikov integral calculation in [8]: the Melnikov integral has the same nonzero sign at any front. Earlier proofs using shooting were given in [14, 15]. We denote the speed of the traveling front by $\sigma(\beta, \bar{u}_1)$; from the fact that the Melnikov integral is nonzero, it is a smooth function.

For finite Lewis number ($\kappa > 0$), there are the following existence and uniqueness results. The papers [3] and [16] use the system (2.1)–(2.2); we have converted their results into results for the system (1.1)–(1.2).

(1) $\kappa = 1$, $\bar{u}_1 = 0$: the system reduces to one second-order equation, and existence is proved by phase plane analysis [4]. The same proof would work for $0 < \bar{u}_1 < \beta^{-1}$. For $0 < \bar{u}_1 < \beta^{-1}$, uniqueness is shown in [3].
(2) $\kappa > 0$, $0 < \bar{u}_1 < \beta^{-1}$: proof of existence by Leray-Schauder degree [3]. For $0 < \kappa < 1$, uniqueness is shown in [16].
(3) $\kappa > 0$, $\bar{u}_1 = 0$: proof of existence by Leray-Schauder degree [16].
(4) $\kappa > 0$ small, $\bar{u}_1 = 0$: proof of existence and uniqueness by geometric singular perturbation theory [7]. The same proof would work for $0 < \bar{u}_1 < \beta^{-1}$. This method of proof also shows that the speed of the traveling wave for small κ is close to that for $\kappa = 0$, and in fact is a smooth function of $(\beta, \bar{u}_1, \kappa)$ for $\beta > 0$, $0 \leq \bar{u}_1 < \beta^{-1}$, and $0 \leq \kappa < \kappa_0(\beta, \bar{u}_1)$ for some positive function κ_0.

2.1.2. *Stability.* For $\bar{u}_1 = 0$, it is shown in [8] for $\kappa = 0$ and in [6] for small $\kappa > 0$ that the front is nonlinearly stable in an appropriate sense, provided the Evans function has no zeros in $\operatorname{Re}\lambda \geq 0$ other than a simple zero at the origin. The same proof would work for $0 < \bar{u}_1 < \beta^{-1}$. Simplicity of the zero at the origin is a consequence of the fact that the Melnikov integral mentioned above is nonzero; equivalently, it is a consequence of the nondegenerate splitting of invariant manifolds that occurs in the construction of the front.

Numerical computation with $\bar{u}_1 = 0$ indicates that the Evans function condition holds for β not too large (for $\kappa = 0$ see [8], for $\kappa > 0$ see [11, 2]). However, for larger β, the wave becomes unstable due to a pair of eigenvalues crossing into the right half-plane [11, 2].

2.2. **Literature on traveling combustion fronts for (1.1)–(1.2) with heat loss ($\delta > 0$).** For $\delta > 0$, spatially homogeneous equilibria of (1.1)–(1.2) all have temperature u_1 equal to 0. We consider fronts with values $(u_1, u_2) = (0, u_2^*)$ at the left and $(u_1, u_2) = (0, 1)$ at the right, where u_2^*, the concentration of unburned reactant behind the front, must be determined.

2.2.1. *Infinite Lewis number ($\kappa = 0$).* We found no results in the literature.

2.2.2. *Finite Lewis number ($\kappa > 0$).* Existence:

(1) For the system (2.3)–(2.4) with ϵ small, $\kappa = 1$, and $\bar{u}_1 > 0$: proof of existence of two solutions for small $\hat{\delta}$ by Leray-Schauder degree [5].
(2) For the system (1.1)–(1.2) with $\beta = 1$, $\kappa > 0$, and $\bar{u}_1 > 0$: proof of existence of two solutions for small δ by Leray-Schauder degree [17].

Numerical results: Figure 5 in [20], which uses the system (2.3)–(2.4), is typical of the numerical results in the literature. For $(\epsilon, \bar{u}_1) = (0.1, 0)$, it shows the wave speed plotted against $\hat{\delta}$ for different values of $\kappa > 0$. For $\hat{\delta}$ small there two traveling waves; they meet in a saddle-node bifurcation at some $\hat{\delta} = \hat{\delta}_0$, and there are no traveling waves for $\hat{\delta} > \hat{\delta}_0$. As $\hat{\delta} \to 0$ the two speeds appear to approach 0 and the speed of the combustion front for $\hat{\delta} = 0$.

Spectral stability: see the review article [20], which uses the form (2.3)–(2.4).

(1) Essential spectrum: At both ends of the wave, the spectrum of the corresponding constant-coefficient operator lies in the left half-plane but touches the imaginary axis. See Figure 6 in [20].
(2) Discrete spectrum: Determined using the Evans function. A typical result is shown in Figure 9 in [20], reproduced here as Figure 2.1. The figure shows, for $(\epsilon, \bar{u}_1, \kappa) = (0.1, 0, 0.5)$, the curve in $\hat{\delta}\hat{\sigma}$-space ($\hat{\sigma}$ = wave speed) for which traveling waves exist. On the upper part of the curve ($\hat{\delta}$ small, $\hat{\sigma}$ near the speed of the traveling wave for $\hat{\delta} = 0$) all eigenvalues except for 0 lie in the left half-plane. At a point marked H on the upper part of the curve a pair of complex eigenvalues crosses into the right half-plane. Thereafter the traveling waves are unstable. However, as one moves along the curve, these eigenvalues become real, and then, at the saddle-node bifurcation point (see p. 27), one of these real eigenvalues crosses back over the imaginary axis.

Figure 5 in [20] shows how this bifurcation diagram changes as κ varies with ϵ held fixed. As κ increases (L_A decreases), H and the saddle-node bifurcation point come together in a Takens-Bogdanov point. After that the saddle-node bifurcation point is still present but H is not. Above the saddle-node bifurcation point all eigenvalues except for 0 lie in the left half-plane, and at the saddle-node bifurcation point, one crosses into the right-half plane.

On the other hand, as κ decreases (L_A increases), eventually H moves left to $\hat{\delta} = 0$. For lower κ (higher L_A) all traveling waves are unstable.

For ϵ near 0, this whole picture can be derived asymptotically REFERENCE.

The fact that for $\epsilon = 0.1$ and small κ, all traveling waves are unstable, is consistent with [11], in which it is found that for $\delta = 0$ and κ small, the combustion front, which is stable for small β, loses stability in a Hopf bifurcation when β increases past about 7 (or when ϵ fall below about 0.14).

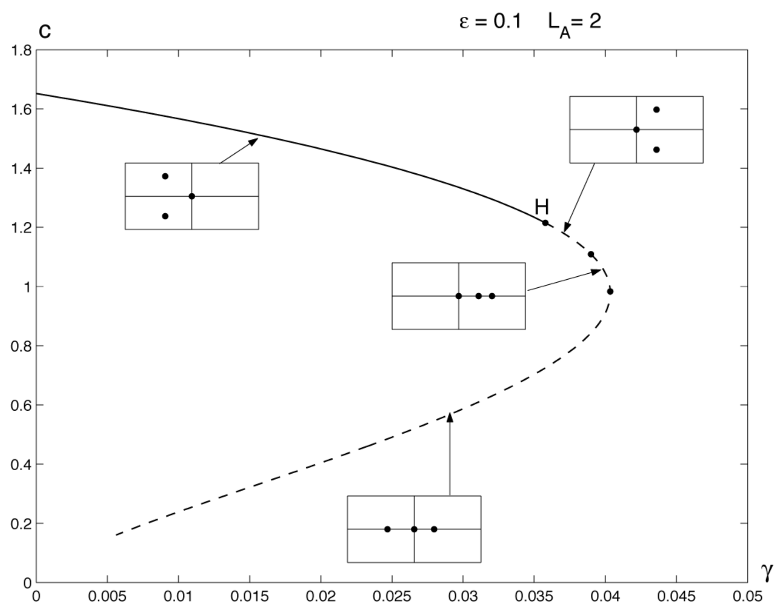

FIGURE 2.1. Figure 9 of [20], showing, for the system (2.3)–(2.4) with $\epsilon = 0.1$, $\bar{u}_1 = 0$, and $\kappa = L_A^{-1} = 0.5$, the curve in $\hat{\delta}\hat{\sigma}$-space ($\hat{\sigma}$ = wave speed) for which traveling waves exist. In the figure, γ corresponds to our $\hat{\delta}$ and c to our $\hat{\sigma}$.

For β below about 7 and κ small, the traveling wave is stable for $\delta = 0$, and, as in Figure 2.1, we would find stability on the upper branch, at least near $\delta = 0$.

It appears that for all (β, κ) that have been studied, the traveling waves with δ below the saddle-node bifurcation value are unstable.

Linearized and nonlinear stability: not discussed in the literature.

3. Existence of traveling waves with speed of order one

In (1.1)–(1.2), we replace the spatial coordinate x with one ξ that is moving with velocity σ: $\xi = x - \sigma t$. We obtain

$$\partial_t u_1 = \partial_{\xi\xi} u_1 + \sigma \partial_\xi u_1 + u_2 \rho(u_1 - \bar{u}_1) - \delta u_1, \tag{3.1}$$

$$\partial_t u_2 = \kappa \partial_{\xi\xi} u_2 + \sigma \partial_\xi u_2 - \beta u_2 \rho(u_1 - \bar{u}_1). \tag{3.2}$$

A steady solution of (3.1)–(3.2) is a traveling wave solution of (1.1)–(1.2) with velocity σ. Steady solutions of (3.1)–(3.2) satisfy the system of ODEs

$$0 = \partial_{\xi\xi} u_1 + \sigma \partial_\xi u_1 + u_2 \rho(u_1 - \bar{u}_1) - \delta u_1, \tag{3.3}$$

$$0 = \kappa \partial_{\xi\xi} u_2 + \sigma \partial_\xi u_2 - \beta u_2 \rho(u_1 - \bar{u}_1). \tag{3.4}$$

3.1. **Infinite Lewis number ($\kappa = 0$), no heat loss ($\delta = 0$).** This section should be regarded as a review.

We consider (3.3)–(3.4) with $(\beta, \bar{u}_1)$ fixed and $\delta = \kappa = 0$. We are interested in solutions with $\sigma > 0$ that satisfy the boundary conditions

$$(u_1, \partial_\xi u_1, u_2)(-\infty) = (u_1^*, 0, 0), \quad (u_1, \partial_\xi u_1, u_2)(\infty) = (0, 0, 1). \tag{3.5}$$

The temperature of combustion $u_1^* > \bar{u}_1$ and the speed $\sigma > 0$ are yet to be determined. In addition we require that the solution approach its end states exponentially.

In the system (3.3)–(3.4) with $\delta = \kappa = 0$, we set $v_1 = \partial_\xi u_1$ and use prime to denote derivative with respect to ξ. We obtain the first-order system

$$u_1' = v_1, \tag{3.6}$$

$$v_1' = -\sigma v_1 - u_2\rho(u_1 - \bar{u}_1), \tag{3.7}$$

$$u_2' = \frac{\beta}{\sigma} u_2\rho(u_1 - \bar{u}_1), \tag{3.8}$$

which has the vector of parameters $(\beta, \bar{u}_1, \sigma)$. A solution of (3.3)–(3.4) that satisfies the boundary conditions (3.5) corresponds to a solution of (3.6)–(3.8) that goes from an equilibrium $(u_1^*, 0, 0)$ to the equilibrium $(0, 0, 1)$.

The set of equilibria of (3.6)–(3.8) is the half plane $H_{\bar{u}_1} = \{(u_1, v_1, u_2) : u_1 \leq \bar{u}_1 \text{ and } v_1 = 0\}$ together with the ray $R_{\bar{u}_1} = \{(u_1, v_1, u_2) : u_1 > \bar{u}_1 \text{ and } v_1 = u_2 = 0\}$. $H_{\bar{u}_1}$ is normally hyperbolic: the equilibria in $H_{\bar{u}_1}$ have two zero eigenvalues and one negative eigenvalue. $R_{\bar{u}_1}$ is also normally hyperbolic: the equilibria in $R_{\bar{u}_1}$ have one positive and one negative eigenvalue. To find a solution to the boundary value problem that satisfies the exponential approach condition, we need to find a solution in the intersection of $W^u(R_{\bar{u}_1})$, which has dimension 2, and $W^s(0, 0, 1)$, which has dimension 1. Of course these manifolds depend on the vector of parameters $(\beta, \bar{u}_1, \sigma)$.

The function $(u_1, v, u_2) \to \sigma u_1 + v + \frac{\sigma}{\beta} u_2$ is a first integral of (3.6)–(3.8). To take advantage of this fact, we replace v_1 by w_1 defined by $w_1 = \sigma u_1 + v_1 + \frac{\sigma}{\beta} u_2$. In the new variables, the differential equation (3.6)–(3.8) becomes

$$u_1' = -\sigma u_1 + w_1 - \frac{\sigma}{\beta} u_2, \tag{3.9}$$

$$w_1' = 0, \tag{3.10}$$

$$u_2' = \frac{\beta}{\sigma} u_2\rho(u_1 - \bar{u}_1). \tag{3.11}$$

Each plane $w_1 =$ constant is invariant. Corresponding to $H_{\bar{u}_1}$and $R_{\bar{u}_1}$ we have

$$\tilde{H}_{(\beta,\bar{u}_1,\sigma)} = \{(u_1, w_1, u_2) : u_1 \leq \bar{u}_1 \text{ and } u_2 = -\beta u_1 + \frac{\beta}{\sigma} w_1\}, \tag{3.12}$$

$$\tilde{R}_{(\beta,\bar{u}_1,\sigma)} = \{(u_1, w_1, u_2) : u_1 = \frac{1}{\sigma} w_1, w_1 > \sigma\bar{u}_1, \text{ and } u_2 = 0\}. \tag{3.13}$$

For a fixed w_1 with $w_1 > \sigma\bar{u}_1$, the phase portrait of (3.9), (3.11) is shown if Figure 3.1. The half-line of equilibria is part of $\tilde{H}_{(\beta,\bar{u}_1,\sigma)}$, and the isolated equilibrium is part of $\tilde{R}_{(\beta,\bar{u}_1,\sigma)}$. Where the unstable manifold of the isolated equilibrium goes depends on the the vector of parameters $(\beta, \bar{u}_1, \sigma, w_1)$ in (3.9), (3.11).

Set $w_1 = \frac{\sigma}{\beta}$, so that the equilibrium on the u_2 axis is at $u_2 = 1$ as desired. The isolated equilibrium then has $u_1 = \frac{1}{\beta}$, so we assume $\bar{u}_1 < \frac{1}{\beta}$. If we now vary σ, it is not hard to see that for small σ, the unstable manifold of $(\frac{1}{\beta}, 0)$ lies above the stable manifold of $(0, 1)$, and for large σ it lies below [4, 21]. Therefore there is a value σ^* of σ for which the unstable manifold of $(\frac{1}{\beta}, 0)$ meets the stable manifold of $(0, 1)$. A Melnikov integral calculated at any such σ^* has the same nonzero sign [8]. It follows that σ^* is unique, and the intersection breaks in a nondegenerate manner as σ varies. We let $\sigma^* = \sigma(\beta, \bar{u}_1)$; because the Melnikov

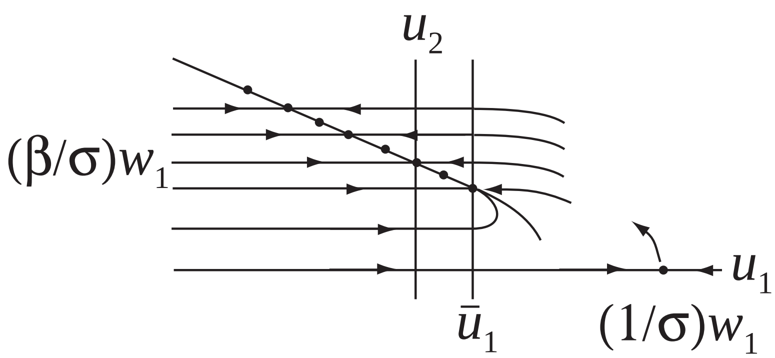

FIGURE 3.1.

integral is nonzero, σ is smooth. For the given $(\beta, \bar{u}_1)$, the heteroclinic solution we have found is the unique traveling wave with positive velocity that satisfies the exponential approach condition, and $\sigma(\beta, \bar{u}_1)$ is its velocity.

This discussion can be reinterpreted as follows. For the system (3.9)–(3.11), with vector of parameters $(\beta, \bar{u}_1, \sigma)$, one can define a separation function $\tilde{S}(\beta, \bar{u}_1, \sigma)$ between the 2-dimensional manifold $W^u(\tilde{R}_{(\beta,\bar{u}_1,\sigma)})$ and the 1-dimensional stable manifold of the equilibrium $(0, \frac{\sigma}{\beta}, 1)$. $\tilde{S} = 0$ when $\sigma = \sigma(\beta, \bar{u}_1)$, and the partial derivative of $\tilde{S}$ with respect to σ there, which is given by the Melnikov integral, is nonzero. When $\tilde{S} = 0$, the two manifolds intersect in a heteroclinic solution from $(\frac{1}{\beta}, \frac{\sigma(\beta,\bar{u}_1)}{\beta}, 0)$ to $(0, \frac{\sigma(\beta,\bar{u}_1)}{\beta}, 1)$.

Returning to $u_1v_1u_2$-space, we have

Theorem 3.1. *For the system* (3.6)–(3.8)*, with vector of parameters* $(\beta, \bar{u}_1, \sigma)$ *and* $\bar{u}_1 < \frac{1}{\beta}$*, one can define a separation function* $S(\beta, \bar{u}_1, \sigma)$ *between the 2-dimensional manifold* $W^u(R_{\bar{u}_1})$ *and the 1-dimensional stable manifold of the equilibrium* $(0, 0, 1)$*.* $S = 0$ *when* $\sigma = \sigma(\beta, \bar{u}_1)$*, and the partial derivative of* S *with respect to* σ *there is nonzero. When* $S = 0$*, the two manifolds intersect in a heteroclinic solution from* $(\frac{1}{\beta}, 0, 0)$ *to* $(0, 0, 1)$*.*

3.2. **Infinite Lewis number ($\kappa = 0$) with heat loss ($\delta > 0$).** We consider (3.3)–(3.4) with $(\beta, \bar{u}_1)$ fixed, $\delta > 0$, and $\kappa = 0$. We are interested in solutions with $\sigma > 0$ that satisfy the boundary conditions

$$(u_1, \partial_\xi u_1, u_2)(-\infty) = (0, 0, u_2^*), \quad (u_1, \partial_\xi u_1, u_2)(\infty) = (0, 0, 1). \tag{3.14}$$

The unburned reactant concentration behind the front u_2^* and the speed σ are yet to be determined.

As in the previous subsection, in the system (3.3)–(3.4) we set $v_1 = \partial_\xi u_1$ and use prime to denote derivative with respect to ξ. We obtain the first-order system

$$u_1' = v_1, \tag{3.15}$$

$$v_1' = -\sigma v_1 - u_2\rho(u_1 - \bar{u}_1) + \delta u_1, \tag{3.16}$$

$$u_2' = \frac{\beta}{\sigma} u_2 \rho(u_1 - \bar{u}_1), \tag{3.17}$$

which has the vector of parameters $(\beta, \bar{u}_1, \sigma, \delta)$. A solution of (3.3)–(3.4) that satisfies the boundary conditions (3.14) corresponds to a solution of (3.15)–(3.17) that goes from an equilibrium $(0, 0, u_2^*)$ to the equilibrium $(0, 0, 1)$.

3.2.1. *Equilibria.* For $\delta > 0$, the set of equilibria of (3.15)–(3.17) is the u_2-axis. The linearization of (3.15)–(3.17) at a point (u_1, v_1, u_2) has the matrix

$$\begin{pmatrix} 0 & 1 & 0 \\ -u_2\rho'(u_1 - \bar{u}_1) + \delta & -\sigma & -\rho(u_1 - \bar{u}_1) \\ \frac{\beta}{\sigma}u_2\rho'(u_1 - \bar{u}_1) & 0 & \frac{\beta}{\sigma}\rho(u_1 - \bar{u}_1) \end{pmatrix} \tag{3.18}$$

On the u_2-axis, (3.18) becomes

$$\begin{pmatrix} 0 & 1 & 0 \\ \delta & -\sigma & 0 \\ 0 & 0 & 0 \end{pmatrix}. \tag{3.19}$$

The characteristic equation is

$$\lambda(\lambda^2 + \sigma\lambda - \delta) = 0, \tag{3.20}$$

so the equilibria all have the eigenvalues

$$0 \quad \text{and} \quad \lambda_\pm(\sigma, \delta) = -\frac{\sigma}{2} \pm \left(\frac{\sigma^2}{4} + \delta\right)^{\frac{1}{2}}. \tag{3.21}$$

Since $\delta > 0$, we have $\lambda_- < 0$ and $\lambda_+ > 0$. Therefore each equilibrium has a one-dimensional unstable manifold and a one-dimensional stable manifold. We need to find a solution that lies in the intersection of the unstable manifold of the u_2-axis, which is two-dimensional, and the stable manifold of $(0, 0, 1)$, which is one-dimensional.

For $\delta = 0$ the equilibria are the half-plane $H_{\bar{u}_1}$, which we now denote $H_{(\beta,\bar{u}_1,\sigma,0)}$ (the last component is δ), and $R_{\bar{u}_1}$; see Figure 3.2 (a).

3.2.2. *Normally hyperbolic invariant manifolds.* For δ=0, the unstable manifolds of points on $R_{\bar{u}_1}$ fit together with the half-plane $H_{(\beta,\bar{u}_1,\sigma,0)}$ to make a normally attracting two-dimensional manifold that we denote $M_{(\beta,\bar{u}_1,\sigma,0)}$. See Figure 3.2 (a).

For small $\delta > 0$, $M_{(\beta,\bar{u}_1,\sigma,0)}$ perturbs to a two-dimensional normally attracting manifold $M_{(\beta,\bar{u}_1,\sigma,\delta)}$. $M_{(\beta,\bar{u}_1,\sigma,\delta)}$ includes the half-plane $H_{(\beta,\bar{u}_1,\sigma,\delta)} = \{(u_1, v_1, u_2) : u_1 \leq \bar{u}_1 \text{ and } v_1 = \lambda_+(\sigma, \delta)u_1\}$, and the line $L_{(\beta,\bar{u}_1,\sigma,\delta)} = \{(u_1, v_1, u_2) : v_1 = \lambda_+(\sigma, \delta)u_1 \text{ and } u_2 = 0\}$. Note that $\lambda_+(\sigma, 0) = 0$, so $L_{(\beta,\bar{u}_1,\sigma,0)}$ contains R_{u_1}. See Figure 3.2 (b).

Explanation of $H_{(\beta,\bar{u}_1,\sigma,\delta)}$: for $u_1 \leq \bar{u}_1$, the plane $v_1 = ku_1$ is invariant provided $v_1' = ku_1'$, i.e., $-\sigma v_1 + \delta u_1 = kv_1$, i.e., $-\sigma k u_1 + \delta u_1 = k^2 u_1$, i.e., $k^2 + \sigma k - \delta = 0$. Compare (3.20). The explanation of $L_{(\beta,\bar{u}_1,\sigma,\delta)}$ is similar.

The differential equation restricted to $H_{(\beta,\bar{u}_1,\sigma,\delta)} \cup L_{(\beta,\bar{u}_1,\sigma,\delta)}$ is just $u_1' = \lambda_+(\delta, \sigma)u_1$, $u_2' = 0$. The u_2-axis, which is contained in $H_{(\beta,\bar{u}_1,\sigma,\delta)}$ and hence in $M_{(\beta,\bar{u}_1,\sigma,\delta)}$, is a normally repelling line of equilibria within $M_{(\beta,\bar{u}_1,\sigma,\delta)}$. In fact $M_{(\beta,\bar{u}_1,\sigma,\delta)}$ is foliated by the unstable manifolds of equilibria on the u_2-axis. The line $L_{(\beta,\bar{u}_1,\sigma,\delta)}$ is the unstable manifold of the origin.

Theorem 3.2. *There is a smooth function $\sigma(\beta, \bar{u}_1, \delta)$, defined for small $\delta \geq 0$, with $\sigma(\beta, \bar{u}_1, 0)$ equal to the function $\sigma(\beta, \bar{u}_1)$ of Theorem 3.1, with the following property. For $\delta > 0$, there is a solution of (3.15)–(3.17) that goes from an equilibrium $(0, 0, u_2^*)$ to the equilibrium $(0, 0, 1)$ and has σ near $\sigma(\beta, \bar{u}_1, 0)$ if and only if $\sigma = \sigma(\beta, \bar{u}_1, \delta)$. Moreover, $u_2^* = u_2^*(\beta, \bar{u}_1, \delta)$ is positive, and $u_2^*(\beta, \bar{u}_1, \delta) \to 0$ as $\delta \to 0$. As $\delta \to 0$, in $u_1v_1u_2$-space the heteroclinic solution*

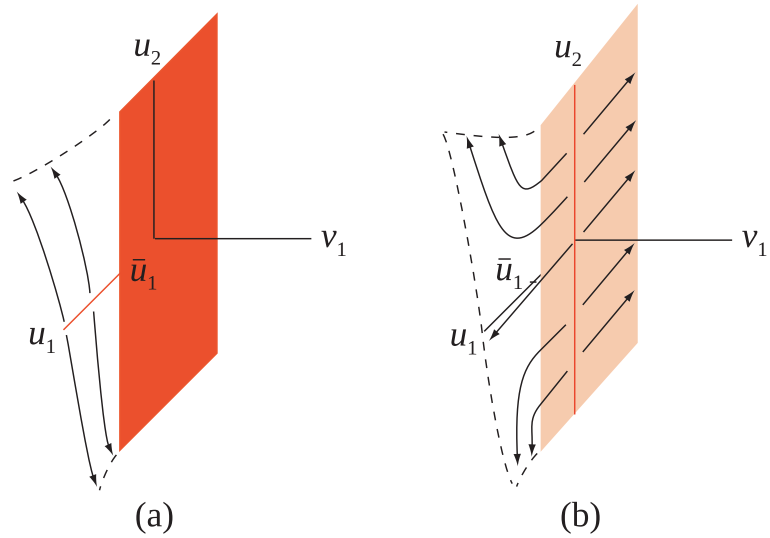

FIGURE 3.2. (a) The two-dimensional normally attracting manifold $M_{(\beta,\bar{u}_1,\sigma,0)}$ for (3.6)–(3.8). It includes the half-plane $H_{(\beta,\bar{u}_1,\sigma,0)}$ of equilibria (red), the ray $R_{\bar{u}_1}$ (part of the u_1-axis) of equilibria (red), and the unstable manifolds of points on $R_{\bar{u}_1}$. (b) The two-dimensional normally attracting manifold $M_{(\beta,\bar{u}_1,\sigma,\delta)}$, $\delta > 0$, for (3.15)–(3.17). It includes the u_2-axis, which is a line of equilibria, and the unstable manifolds of these equilibria. Within the half-plane $H_{(\beta,\bar{u}_1,\sigma,\delta)}$, which is part of $M_{(\beta,\bar{u}_1,\sigma,\delta)}$, the unstable manifolds are parallel lines. The entire unstable manifold of the origin is the line $L_{(\beta,\bar{u}_1,\sigma,\delta)}$, which lies in the plane $u_2 = 0$.

approaches the union of the heteroclinic solution for $(\beta, \bar{u}_1, \sigma, \delta) = (\beta, \bar{u}_1, \sigma(\beta, \bar{u}_1, 0), 0)$ *and the line segment from* $(0, 0, 0)$ *to* $(\frac{1}{\beta}, 0, 0)$.

See Figure 3.3.

To prove the theorem, just note that the separation function $S(\beta, \bar{u}_1, \sigma)$ of Theorem 3.1 extends to a separation function $S(\beta, \bar{u}_1, \sigma, \delta)$ between the two-dimensional manifold $M_{(\beta,\bar{u}_1,\sigma,\delta)}$ and the one-dimensional stable manifold of $(0, 0, 1)$; we have $S(\beta, \bar{u}_1, \sigma, 0)$ equal to the previously defined $S(\beta, \bar{u}_1, \sigma)$. Since $S = 0$ and the partial derivative of S with respect to σ is nonzero at $(\beta, \bar{u}_1, \sigma, \delta)$ with $\sigma = \sigma(\beta, \bar{u}_1)$ and $\delta = 0$, there is a function $\sigma(\beta, \bar{u}_1, \delta)$, with $\delta \geq 0$ small and $\sigma(\beta, \bar{u}_1, 0)$ equal to the previously defined $\sigma(\beta, \bar{u}_1)$, such that $S = 0$ when $\sigma = \sigma(\beta, \bar{u}_1, \delta)$. For such σ, a branch of the stable manifold of $(0, 0, 1)$ lies in $M_{(\beta,\bar{u}_1,\sigma,\delta)}$. Since $M_{(\beta,\bar{u}_1,\sigma,\delta)}$ is foliated by the unstable manifolds of equilibria, in backward time it approaches an equilibrium. That equilibrium cannot be the origin because our solution lies in the invariant set $u_2 > 0$ and the unstable manifold of the origin, $L_{(\beta,\bar{u}_1,\sigma,\delta)}$, lies in the invariant plane $u_2 = 0$.

3.3. **Finite Lewis number ($\kappa > 0$).** The approach of this section was used in [2] and [7] for $\delta = 0$.

We consider (3.3)–(3.4) with $(\beta, \bar{u}_1)$ fixed, $\delta \geq 0$, and $\kappa > 0$. For $\delta = 0$ we use the boundary conditions

$$(u_1, \partial_\xi u_1, u_2, \partial_\xi u_2)(-\infty) = (u_1^*, 0, 0, 0), \quad (u_1, \partial_\xi u_1, u_2, \partial_\xi u_2)(\infty) = (0, 0, 1, 0). \tag{3.22}$$

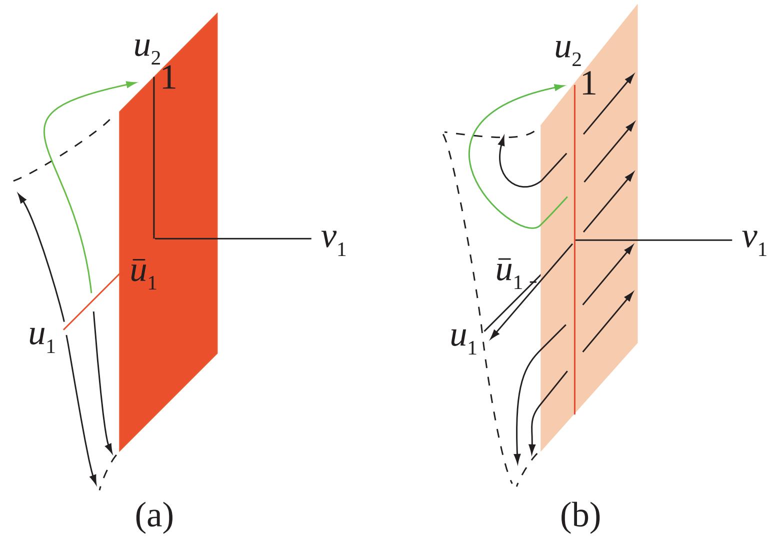

FIGURE 3.3. Invariant manifolds and connecting orbit for $\sigma = \sigma(\beta, \bar{u}_1, \delta)$: (a) $\delta = 0$ and (b) $\delta > 0$.

u_1^* represents the combustion temperature; it and the speed σ are yet to be determined. For $\delta > 0$ we use the boundary conditions

$$(u_1, \partial_\xi u_1, u_2, \partial_\xi u_2)(-\infty) = (0, 0, u_2^*, 0), \quad (u_1, \partial_\xi u_1, u_2, \partial_\xi u_2)(\infty) = (0, 0, 1, 0). \tag{3.23}$$

u_2^* represents the reactant concentration behind the front; it and the speed σ are yet to be determined.

In the system (3.3)–(3.4) we set $v_1 = \partial_\xi u_1$, $v_2 = \partial_\xi u_2$, and use prime to denote derivative with respect to ξ. We obtain the first-order system

$$u_1' = v_1, \tag{3.24}$$

$$v_1' = -\sigma v_1 - u_2 \rho(u_1 - \bar{u}_1) + \delta u_1, \tag{3.25}$$

$$u_2' = v_2, \tag{3.26}$$

$$\kappa v_2' = -\sigma v_2 + \beta u_2 \rho(u_1 - \bar{u}_1). \tag{3.27}$$

This system has the vector of parameters $(\beta, \bar{u}_1, \sigma, \delta, \kappa)$. We restrict our attention to $\kappa > 0$, $\delta \geq 0$, and $\sigma > 0$. For $\kappa > 0$, a solution of (3.3)–(3.4) that satisfies the boundary conditions (3.22) (respectively (3.23)) corresponds to a solution of (3.24)–(3.27) that goes from an equilibrium $(u_1^*, 0, 0, 0)$ (respectively $(0, 0, u_2^*, 0)$) to, in both cases, the equilibrium $(0, 0, 1, 0)$.

For $\kappa > 0$ and $\delta = 0$, the set of equilibria of (3.24)–(3.27) is the half plane $H_{\bar{u}_1} = \{(u_1, v_1, u_2, v_2) : u_1 \leq \bar{u}_1 \text{ and } v_1 = v_2 = 0\}$ together with the ray $R_{\bar{u}_1} = \{(u_1, v_1, u_2, v_2) : u_1 > \bar{u}_1 \text{ and } v_1 = u_2 = v_2 = 0\}$. $H_{\bar{u}_1}$ is normally hyperbolic: the equilibria in $H_{\bar{u}_1}$ have two zero eigenvalues and two negative eigenvalues. $R_{\bar{u}_1}$ is also normally hyperbolic: the equilibria in $R_{\bar{u}_1}$ have one positive and two negative eigenvalue. To solve the boundary value problem (3.24)–(3.27), (3.22), we need to find a solution in the intersection of $W^u(R_{\bar{u}_1})$, which has dimension 2, and $W^s(0, 0, 1)$, which also has dimension 2.

For $\kappa > 0$ and $\delta > 0$, the set of equilibria of (3.24)–(3.27) is the u_2-axis. Linearization shows that each equilibrium has a one-dimensional unstable manifold and a two-dimensional stable manifold. To solve the boundary value problem (3.24)–(3.27), (3.23), we need to find a solution in the intersection of the unstable manifold of the u_2-axis, which has dimension 2, and $W^s(0,0,1)$, which also has dimension 2.

For small $\kappa > 0$, the system (3.24)–(3.27) may be regarded as the slow form of a slow-fast system. The fast form is obtained by multiplying the right-hand side by κ:

$$\dot{u}_1 = \kappa v_1, \tag{3.28}$$

$$\dot{v}_1 = \kappa\big(-\sigma v_1 - u_2\rho(u_1 - \bar{u}_1) + \delta u_1\big), \tag{3.29}$$

$$\dot{u}_2 = \kappa v_2, \tag{3.30}$$

$$\dot{v}_2 = -\sigma v_2 + \beta u_2 \rho(u_1 - \bar{u}_1). \tag{3.31}$$

For $\kappa = 0$, the set of equilibria of (3.28)–(3.31) is the 3-dimensional manifold (slow manifold)

$$P_{(\beta,\bar{u}_1,\sigma,\delta,0)} = (\{(u_1, v_1, u_2, v_2) : v_2 = \frac{\beta}{\sigma} u_2 \rho(u_1 - \bar{u}_1)\}.$$

These equilibria have the eigenvalues 0 with multiplicity 3 and $-\sigma$, so the slow manifold is normally attracting. It is parameterized by (u_1, v_1, u_2). The slow system on the slow manifold ((3.24)–(3.26) with $v_2 = \frac{\beta}{\sigma} u_2 \rho(u_1 - \bar{u}_1)$) is given by (3.15)–(3.17).

For small $\kappa > 0$, $P_{(\beta,\bar{u}_1,\sigma,\delta,0)}$ perturbs to a normally attracting manifold $P_{(\beta,\bar{u}_1,\sigma,\delta,\kappa)}$. The differential equation on $P_{(\beta,\bar{u}_1,\sigma,\delta,\kappa)}$, divided by κ, is a perturbation of (3.15)–(3.17).

The 2-dimensional manifold $M_{(\beta,\bar{u}_1,\sigma,\delta)}$ of the previous subsection, and the one-dimensional stable manifold of (0,0,1) used in that subsection, correspond to submanifolds of $P_{(\beta,\bar{u}_1,\sigma,\delta,0)}$ that we denote $M_{(\beta,\bar{u}_1,\sigma,\delta,0)}$ and $N_{(\beta,\bar{u}_1,\sigma,\delta,0)}$.

For small $\kappa > 0$, these manifolds perturb to invariant manifolds $M_{(\beta,\bar{u}_1,\sigma,\delta,\kappa)}$ and $N_{(\beta,\bar{u}_1,\sigma,\delta,\kappa)}$ of $P_{(\beta,\bar{u}_1,\sigma,\delta,\kappa)}$. $M_{(\beta,\bar{u}_1,\sigma,\delta,\kappa)}$ contains:

- for $\delta = 0$, the 2-dimensional unstable manifold of the ray $R_{\bar{u}_1}$ of equilibria;
- for $\delta > 0$, the 2-dimensional unstable manifold of the u_2-axis.

$N(\beta, \bar{u}_1, \sigma, \delta, \kappa)$ is a 1-dimensional portion of the 2-dimensional stable manifold of $(0,0,0,1)$.

The separation function $S(\beta, \bar{u}_1, \sigma, \delta)$ used in the proof of Theorem 3.2 extends to a separation function $S(\beta, \bar{u}_1, \sigma, \delta, \kappa)$ between $M_{(\beta,\bar{u}_1,\sigma,\delta,\kappa)}$ and $N_{(\beta,\bar{u}_1,\sigma,\delta,\kappa)}$; we have $S(\beta, \bar{u}_1, \sigma, \delta, 0)$ equal to the previously defined $S(\beta, \bar{u}_1, \sigma, \delta)$. Since $S = 0$ and the partial derivative of S with respect to σ is nonzero at $(\beta, \bar{u}_1, \sigma, \delta, \kappa)$ with $\sigma = \sigma(\beta, \bar{u}_1, \delta)$ and $\kappa = 0$, there is a function $\sigma(\beta, \bar{u}_1, \delta, \kappa)$, with $\kappa \geq 0$ small and $\sigma(\beta, \bar{u}_1, \delta, 0)$ equal to the previously defined $\sigma(\beta, \bar{u}_1, \delta)$, such that $S = 0$ when $\sigma = \sigma(\beta, \bar{u}_1, \delta, \kappa)$. For such σ, $N_{(\beta,\bar{u}_1,\sigma,\delta,\kappa)}$ lies in $M_{(\beta,\bar{u}_1,\sigma,\delta,\kappa)}$.

For $\delta > 0$, $\kappa > 0$, and such σ, in backward time $N_{(\beta,\bar{u}_1,\sigma,\delta,\kappa)}$ approaches an equilibrium, since $M_{(\beta,\bar{u}_1,\sigma,\delta,\kappa)}$ is foliated by the unstable manifolds of equilibria, That equilibrium cannot be the origin because it is easy to see that the unstable manifold of the origin lies in the invariant set $u_2 = v_2 = 0$.

We have proved:

Theorem 3.3. *There is a smooth function $\sigma(\beta, \bar{u}_1, \delta, \kappa)$, defined for small $\delta \geq 0$ and small $\kappa \geq 0$, with $\sigma(\beta, \bar{u}_1, \delta, 0)$ equal to the function $\sigma(\beta, \bar{u}_1, \delta)$ in Theorem 3.2, with the following property. For $\kappa > 0$ and $\delta = 0$, there is a solution of (3.24)–(3.27) that goes from an equilibrium $(u_1^*, 0, 0, 0)$ to the equilibrium $(0, 0, 1, 0)$ and has σ near $\sigma(\beta, \bar{u}_1, 0, 0)$ if and only if $\sigma = \sigma(\beta, \bar{u}_1, 0, \kappa)$. For $\kappa > 0$ and $\delta > 0$, there is a solution of (3.24)–(3.27) that goes from an equilibrium $(0, 0, u_2^*, 0)$ to the equilibrium $(0, 0, 1, 0)$ and has σ near $\sigma(\beta, \bar{u}_1, \delta, 0)$ if and only if $\sigma = \sigma(\beta, \bar{u}_1, \delta, \kappa)$. Moreover, $u_2^* > 0$.*

Remark 3.4. There is considerable numerical evidence, such as Figure 2.1, showing that for δ positive and small there, is a traveling wave with speed near zero. So far as we know, there is no theoretical analysis of the asymptotic behavior of this wave as $\delta \to 0$ with $(\beta, \bar{u}_1, \kappa)$ fixed.

4. Stability of the traveling waves

For $\delta = 0$, we refer to [8] for $\kappa = 0$ and to [6] for $\kappa > 0$, although the proof given below would work for $\delta = 0$ as well with small changes.

Fix $(\beta, \bar{u}_1, \delta, \kappa)$ with $\delta > 0$. Let $(u_{1*}, u_{2*})(\xi)$ be a solution of (3.3)-(3.4), with $\sigma = \sigma(\beta, \bar{u}_1, \delta, \kappa)$, and with boundary values given by (3.14) when $\kappa = 0$ and by (3.23) when $\kappa > 0$.

In order to study the stability of this traveling wave using the theory of [10], we must first shift its left state to the origin.

To do this, let $z_2 = u_2 - u_2^*$. The PDE system (3.1)–(3.2) becomes

$$\partial_t u_1 = \partial_{\xi\xi} u_1 + \sigma \partial_\xi u_1 + (u_2^* + z_2)\rho(u_1 - \bar{u}_1) - \delta u_1, \tag{4.1}$$

$$\partial_t z_2 = \kappa \partial_{\xi\xi} z_2 + \sigma \partial_\xi z_2 - \beta(u_2^* + z_2)\rho(u_1 - \bar{u}_1). \tag{4.2}$$

We write (4.1)–(4.2) as $Y_t = DY_{\xi\xi} + \sigma Y_\xi + R(Y)$ with

$$Y = \begin{pmatrix} u_1 \\ z_2 \end{pmatrix}, \quad D = \begin{pmatrix} 1 & 0 \\ 0 & \kappa \end{pmatrix}, \quad R\begin{pmatrix} u_1 \\ z_2 \end{pmatrix} = \begin{pmatrix} (u_2^* + z_2)\rho(u_1 - \bar{u}_1) - \delta u_1 \\ -\beta(u_2^* + z_2)\rho(u_1 - \bar{u}_1) \end{pmatrix}.$$

Note that $R(0, z_2) \equiv 0$ but $R(u_1, 0)$ is not identically 0.

Let $z_{2*}(\xi) = u_{2*}(\xi) - u_2^*$. Then $Y_*(\xi) = (u_{1*}, z_{2*})(\xi)$ is an equilibrium solution of (4.1)–(4.2), with $Y_*(-\infty) = Y_- = (0, 0)$ and $Y_*(\infty) = Y_+ = (0, 1 - u_2^*)$.

4.1. Rate of approach of $Y_*(\xi)$ to end states.

Recall the numbers $\lambda_\pm(\sigma, \delta)$ given by (3.21). There is a number $K > 0$ such that for $\xi \leq 0$, $\|Y_*(\xi)\| \leq Ke^{\lambda_+(\sigma,\delta)\xi}$. In the case $\kappa = 0$, K can be chosen so that

$$\text{for } \xi \geq 0,\ \|Y_*(\xi) - Y_+\| \leq Ke^{\lambda_-(\sigma,\delta)\xi}. \tag{4.3}$$

In the case $\kappa > 0$, we want the same estimate, but some discussion is required.

For $\kappa > 0$, the traveling wave equation is (3.24)–(3.27). The eigenvalues of the linearization at any equilibrium are $\lambda_\pm(\sigma, \delta)$, 0, and $-\frac{\sigma}{\kappa}$. We have $\lambda_-(\sigma, \delta) < 0 < \lambda_+(\sigma, \delta)$, and for κ sufficiently small,

$$-\frac{\sigma}{\kappa} < \lambda_-(\sigma, \delta). \tag{4.4}$$

We shall assume that (4.4) holds; small changes in our results and their proofs would be required if it does not.

For $\kappa > 0$, if we assume (4.4), then it is reasonable to assume that K can be chosen so that (4.3) holds. We shall assume (4.3); it is in fact true for the traveling waves constructed in subsection 3.3 for small $\kappa > 0$.

4.2. Linearization.

The linearization of (4.1)–(4.2) at $Y_*(\xi)$ is

$$\tilde{Y}_t = L\tilde{Y} = D\tilde{Y}_{\xi\xi} + \sigma\tilde{Y}_\xi + DR(Y_*(\xi))\tilde{Y}.$$

Note that $DR(Y_\pm)\tilde{Y} = \operatorname{diag}(-\delta, 0)\tilde{Y}$, so the linearization of (4.1)–(4.2) at the constant solutions $Y_\pm$ is just

$$\tilde{Y}_t = L^\pm\tilde{Y} = D\tilde{Y}_{\xi\xi} + \sigma\tilde{Y}_\xi + \operatorname{diag}(-\delta, 0)\tilde{Y},$$

so $L^- = L^+$.

We shall refer to "L on L^2" when we should more properly say "the operator defined by L on $L^2(\mathbb{R})$, with its natural domain," etc.

The spectrum of $L^\pm$ on L^2 (and hence on H^1 or on BUC, the space of bounded uniformly continuous functions with the sup norm) can be computed by Fourier transform. It is the union of two curves, $\{\lambda = \theta + i\omega : \theta = -\left(\frac{\omega}{\sigma}\right)^2 - \delta\}$, which is the spectrum of $\partial_{\xi\xi} + \sigma\partial_\xi - \delta$, and $\{\lambda = \theta + i\omega : \theta = -\kappa\left(\frac{\omega}{\sigma}\right)^2\}$, which is the spectrum of $\kappa\partial_{\xi\xi} + \sigma\partial_\xi$. The right-hand boundary of this set of two curves is the right-hand boundary of the essential spectrum of L on L^2 or BUC.

4.3. **Weighted spaces.** Given $\alpha = (\alpha_-, \alpha_+) \in \mathbb{R}^2$, let $\gamma_\alpha(\xi)$ be a smooth positive function that equals $e^{\alpha_-\xi}$ for $\xi \leq -1$ and equals $e^{\alpha_+\xi}$ for $\xi \geq 1$. As in the Introduction, let $\mathcal{E}_0$ denote H^1 or BUC, with norm (the "unweighted norm") $\|\ \|_0$. Let $\mathcal{E}_\alpha$ denote the corresponding weighted space with weight function γ_α: $u \in \mathcal{E}_\alpha$ if and only if $\gamma_\alpha(\xi)u(\xi) \in \mathcal{E}_0$, and $\|u\|_\alpha = \|\gamma_\alpha(\xi)u(\xi)\|_0$. (This definition of $\mathcal{E}_\alpha$ is a little more general than that used in the Introduction.)

Lemma 4.1. *Consider the system (4.1)–(4.2) with $\delta > 0$, $\kappa \geq 0$, and $\sigma = \sigma(\beta, \bar{u}_1, \delta, \kappa)$. Assume (4.3) and (4.4). Suppose $0 < \alpha_- < \lambda_+(\sigma, \delta)$ and $0 < \alpha_+ < -\lambda_-(\sigma, \delta)$. Then the essential spectrum of L on $\mathcal{E}_\alpha$ is contained in a half-plane $\operatorname{Re}\lambda \leq -\nu < 0$.*

The choice of $\alpha_\pm$ in the lemma is motivated by what is needed to use the theory of [10], in light of the previous subsection.

The proof of the lemma is a calculation. The operator L on $\mathcal{E}_\alpha$ is similar to the operator $\gamma_\alpha L \gamma_\alpha^{-1}$ on $\mathcal{E}_0$, and hence has the same spectrum. The latter is given by

$$\hat{L}W = \gamma_\alpha L \gamma_\alpha^{-1} W. \tag{4.5}$$

Setting $\xi = \pm\infty$ in (4.5) yields

$$\hat{L}^\pm W = \begin{pmatrix} \partial_{\xi\xi} + (\sigma - 2\alpha_\pm)\partial_\xi + (\alpha_\pm^2 - \sigma\alpha_\pm - \delta) & 0 \\ 0 & \kappa\partial_{\xi\xi} + (\sigma - 2\kappa\alpha_\pm)\partial_\xi + (\kappa\alpha_\pm^2 - \sigma\alpha_\pm) \end{pmatrix} W.$$

The spectrum of $\hat{L}^-$ on $\mathcal{E}_0$ is the union of two curves, $\{\lambda = \theta + i\omega : \theta = -\left(\frac{\omega}{\sigma - 2\alpha_-}\right)^2 + (\alpha_-^2 - \sigma\alpha_- - \delta)$, which is the spectrum of $\partial_{\xi\xi} + (\sigma - 2\alpha_-)\partial_\xi + (\alpha_-^2 - \sigma\alpha_- - \delta)$, and $\{\lambda = \theta + i\omega : \theta = -\kappa\left(\frac{\omega}{\sigma - 2\alpha_-}\right)^2 + (\kappa\alpha_-^2 - \sigma\alpha_-)$, which is the spectrum of $\kappa\partial_{\xi\xi} + (\sigma - 2\kappa\alpha_-)\partial_\xi + (\kappa\alpha_-^2 - \sigma\alpha_-)$. An analogous result holds for the spectrum of $\hat{L}^+$ on $\mathcal{E}_0$.

From the choice of $\alpha_\pm$ in the lemma, we have

$$0 < \alpha_- < \lambda_+(\sigma, \delta) = -\frac{\sigma}{2} + \left(\frac{\sigma^2}{4} + \delta\right)^{\frac{1}{2}}, \tag{4.6}$$

$$0 < \alpha_+ < -\lambda_-(\sigma, \delta) = \frac{\sigma}{2} + \left(\frac{\sigma^2}{4} + \delta\right)^{\frac{1}{2}}. \tag{4.7}$$

If $\kappa > 0$, (4.4) implies

$$\alpha_- < \lambda_+(\sigma, \delta) < -\lambda_-(\sigma, \delta) < \frac{\sigma}{\kappa} \quad \text{and} \quad \alpha_+ < -\lambda_-(\sigma, \delta) < \frac{\sigma}{\kappa}. \tag{4.8}$$

Therefore $\kappa\alpha_-^2 - \sigma\alpha_- < 0$ and $\kappa\alpha_+^2 - \sigma\alpha_- < 0$. Of course these statements are also true when $\kappa = 0$. Therefore:

(1) If (4.6) holds, then the spectrum of $\hat{L}^-$ on $\mathcal{E}_0$ lies in $\operatorname{Re}\lambda \le \max(\alpha_-^2 - \sigma\alpha_- - \delta, \kappa\alpha_-^2 - \sigma\alpha_-) < 0$.

(2) If (4.7) holds, then the spectrum of $\hat{L}^+$ on $\mathcal{E}_0$ lies in $\operatorname{Re}\lambda \le \max(\alpha_+^2 - \sigma\alpha_+ - \delta, \kappa\alpha_+^2 - \sigma\alpha_+) < 0$.

The lemma follows.

4.4. **Results.** Our stability result is:

Theorem 4.2. *Consider the system* (4.1)–(4.2) *with* $\delta > 0$, $\kappa \ge 0$, *and* $\sigma = \sigma(\beta, \bar{u}_1, \delta, \kappa)$. *Assume* (4.3) *and* (4.4). *Let* α_- *and* α_+ *be chosen as in Lemma 4.1. Let* $\alpha = (\alpha_-, \alpha_+)$ *and let* $\eta = (0, \alpha_+)$. *Assume in addition that the Evans function for the traveling wave* $Y_*(\xi)$ *has no zeros in the half-plane* $\operatorname{Re}\lambda \ge 0$ *other than a simple zero at the origin. Suppose* $Y^0 \in Y_* + \mathcal{E}_\eta^2$ *with* $\|Y^0 - Y_*\|_\eta$ *small, and let* $Y(t)$ *be the solution of* (4.1)–(4.2) *in* $Y_* + \mathcal{E}_\eta^2$ *with* $Y(0) = Y^0$. *Then:*

(1) $Y(t)$ *is defined for all* $t \ge 0$.

(2) $Y(t) = \tilde{Y}(t) + Y_*(\xi - q(t))$ *with* $\tilde{Y}(t)$ *in a fixed subspace of* $\mathcal{E}_\eta^2$ *complementary to the span of* Y_*'. *Let* $\tilde{Y}(t) = (\tilde{u}_1(t), \tilde{z}_2(t))$.

(3) $\|\tilde{Y}(t)\|_\eta + |q(t)|$ *is small for all* $t \ge 0$.

(4) $\|\tilde{Y}(t)\|_\alpha$ *decays exponentially as* $t \to \infty$.

(5) *There exists* q^* *such that* $|q(t) - q^*|$ *decays exponentially as* $t \to \infty$.

(6) *There is a constant* C *independent of* Y^0 *such that* $\|\tilde{z}_2(t)\|_0 \le C\|\tilde{Y}^0\|_\eta$ *for all* $t \ge 0$.

(7) $\|\tilde{u}_1(t)\|_0$ *decays exponentially as* $t \to \infty$.

This theorem follows from the previous subsections and Theorem 3.14 in [10], once note that:

(1) $R(0, z_2) \equiv 0$ (noted at the end of Subsection 4.1).

(2) The operator $\kappa\partial_{\xi\xi} + \sigma\partial_\xi$ on $\mathcal{E}_0$ generates a bounded semigroup.

(3) The operator $\partial_{\xi\xi} + \sigma\partial_\xi - \delta$ on $\mathcal{E}_0$ has its spectrum contained in $\operatorname{Re}\lambda \le -\delta < 0$.

We remark that for a fixed $\delta > 0$, if the Evans function condition in Theorem 4.2 holds for $\kappa = 0$, then it holds for small $\kappa > 0$. The analogous fact for $\delta = 0$ is proved in [7]. The proof for $\delta > 0$ is similar but easier. For $\delta = \kappa = 0$, at the left state of the traveling wave, one spectral curve passes through 0, and at the right state, two do. For $\delta > 0$ and $\kappa = 0$, at each end state of the traveling wave, one spectral curve passes through 0.

Theorem 3.16 in [10] implies some additional conclusions when $\kappa > 0$ in Theorem 4.2. Consider the Banach space $\mathcal{E}_0 \cap L^1(\mathbb{R})$ with the norm $\|u\|_{\mathcal{E}_0 \cap L^1(\mathbb{R})} = \max\{\|u\|_{\mathcal{E}_0}, \|u\|_{L^1(\mathbb{R})}\}$. Suppose $Y^0 \in Y_* + (\mathcal{E}_\eta \cap L^1(\mathbb{R}))^2$ with $\|Y^0 - Y_*\|_\eta$ and $\|Y^0 - Y_*\|_{L^1}$ sufficiently small, and as in Theorem 4.2 let $Y(t)$ be the solution of (4.1)–(4.2) in in $Y_* + \mathcal{E}_\eta^2$ with $Y(0) = Y^0$. Let $h(t) = \min(1, t^{-\frac{1}{2}})$. Then for fixed $\kappa > 0$ and for all $t \ge 0$:

(1) $Y(t) \in (\mathcal{E}_\eta \cap L^1(\mathbb{R}))^2$.

(2) There is a constant C independent of Y^0 such that

$$\|\tilde{z}_2(t)\|_{L^1} \le C \max\left(\|\tilde{z}_2^0)\|_{L^1}, \|\tilde{Y}^0\|_\alpha\right) \quad \text{and} \quad \|\tilde{z}_2\|_{L^\infty} \le Ch(t) \max\left(\|\tilde{z}_2^0\|_{L^1}, \|\tilde{Y}^0\|_\eta\right).$$

(3) $\|\tilde{u}_1\|_{L^1}$ decays exponentially as $t \to \infty$.

5. Evans function

We continue to assume (4.3) and (4.4), and that α_- and α_+ are chosen as in Lemma 4.1.

5.1. **Derivative at 0.** For fixed $(\beta, \bar{u}_1, \delta, \kappa)$ with $\kappa > 0$, we write the traveling wave system (3.24)–(3.27) as $X_\xi = F(X, \sigma)$. Let $X_*(\xi) = (u_{1*}, \dot{u}_{1*}, u_{2*}, \dot{u}_{2*})(\xi)$, with velocity $\sigma_* = \sigma(\beta, \bar{u}_1, \delta, \kappa)$, and let $B(\xi) = F_X(X_*(\xi), \sigma_*)$. (The dot denotes derivative with respect to ξ.)

The complex number λ is an eigenvalue of L on $\mathcal{E}_\alpha$ with eigenfunction $\tilde{Y}$ provided $\tilde{Y} \in \mathcal{E}_\alpha^2$ and $\lambda\tilde{Y} = L\tilde{Y}$. This second-order linear differential equation can be written as the first-order system on $\mathbb{R}^4$

$$X_\xi = (B(\xi) + \lambda C)X, \tag{5.1}$$

with C a constant matrix. X is a solution of (5.1) in $\mathcal{E}_\alpha^4$ if and only if the first and third components of X give a solution $\tilde{Y}$ of $\tilde{Y}_t = L\tilde{Y}$ in $\mathcal{E}_\alpha^2$.

Let

$$\omega_- = \frac{1}{2}\max(\alpha_-^2 - \sigma\alpha_- - \delta, \kappa\alpha_-^2 - \sigma\alpha_-) < 0, \quad \omega_+ = \frac{1}{2}\max(\alpha_+^2 - \sigma\alpha_+ - \delta, \kappa\alpha_+^2 - \sigma\alpha_+) < 0.$$

For $\operatorname{Re}\lambda \geq \omega_-$, (5.1) has linear independent solutions $X^1(\xi,\lambda)$ and $X^2(\xi,\lambda)$ such that $e^{\alpha_-\xi}X^i(\xi)$, $i = 1, 2$, is bounded for $\xi \leq 0$. Similarly, for $\operatorname{Re}\lambda \geq \omega_+$, (5.1) has linear independent solutions $X^3(\xi,\lambda)$ and $X^4(\xi,\lambda)$ such that $e^{\alpha_+\xi}X^i(\xi)$, $i = 3, 4$, is bounded for $\xi \geq 0$. By a theorem of Kato [13], these solutions may be chosen to depend analytically on λ. The Evans function $D(\lambda)$ is defined for $\operatorname{Re}\lambda \geq \max(\omega_-, \omega_+)$ by

$$D(\lambda) = \det\left(X^1(0,\lambda), \dots, X^4(0,\lambda)\right).$$

It is 0 if and only if λ is an eigenvalue of L on $\mathcal{E}_\alpha$.

Let us assume that along $X_*(\xi)$, the two-dimensional tangent spaces to $M_{(\beta,\bar{u}_1,\sigma^*,\delta,\kappa)}$ (defined in subsection 3.3) and to the stable manifold of $(0, 0, 0, 1)$ have just a one-dimensional intersection. (Subsection 3.3 shows that this is true for small $\delta \geq 0$ and small $\kappa > 0$.) Then the $X^i(\xi, 0)$ span a space of dimension 3, and they can be chosen so that $X^1(\xi, 0) = X^3(\xi, 0) = \dot{X}_*(\xi)$, which we assume. Hence up to scalar multiplication there is a unique solution $\psi_*(\xi)$ in $\mathcal{E}^4_{(-\alpha_+,-\alpha_-)}$ of the adjoint equation $\psi_\xi = -B(\xi)^\top\psi$. CORRECT SPACES? We have $\psi_*(\xi)^\top X^i(\xi) = 0$ for $i = 1, \dots, 4$, and, according to [18], up to a nonzero multiple,

$$D'(0) = \int_{-\infty}^{\infty} \psi_*(\xi)^\top C\dot{X}_*(\xi)\,d\xi. \tag{5.2}$$

Let us further assume that the derivative of the separation function used in subsection 3.3 with respect to σ is nonzero at $(\beta, \bar{u}_1, \sigma^*, \delta, \kappa)$. (Subsection 3.3 shows that this is true for small $\delta \geq 0$ and small $\kappa > 0$.) Up to a nonzero multiple, its value at σ_* is given by the Melnikov integral

$$M = \int_{-\infty}^{\infty} \psi_*(\xi)^\top F_\sigma(X_*(\xi), \sigma_*)\,d\xi, \tag{5.3}$$

which is therefore nonzero. It is easy to check that

$$C\dot{X}_*(\xi) = -F_\sigma(X_*(\xi), \sigma_*).$$

Since M is nonzero, it follows that $D'(0) \neq 0$, so 0 is a simple zero of the Evans function.

Formula (5.2) is correct despite the 0 eigenvalues at the end states; see [8]. CHECK THIS. Also, (5.3) is indeed the derivative of the separation function despite the 0 eigenvalues, because the end states are independent of σ; see [19].

A similar discussion holds for $\kappa = 0$.

5.2. **Numerics for $\kappa = 0$.** For fixed $(\beta, \bar{u}_1, \delta)$ and $\kappa = 0$, the traveling wave system is (3.15)–(3.17). Following the previous subsection, we write the traveling wave as $X_*(\xi) = (u_{1*}, \dot{u}_{1*}, u_{2*})(\xi)$. In our numerics we take $\bar{u}_1 = 0$. Then the complex number λ is an eigenvalue of L on $\mathcal{E}_\alpha$ provided the first-order system on $\mathbb{R}^3$

$$X_\xi = (B(\xi) + \lambda C)X = \begin{pmatrix} 0 & 1 & 0 \\ \lambda - u_{2*}(\xi)\rho'(u_{1*}(\xi)) + \delta & -\sigma & -\rho(u_{1*}(\xi)) \\ \frac{\beta}{\sigma}u_{2*}(\xi)\rho'(u_{1*}(\xi)) & 0 & \frac{\lambda}{\sigma} + \frac{\beta}{\sigma}\rho(u_{1*}(\xi)) \end{pmatrix} X \tag{5.4}$$

has a solution in $\mathcal{E}^3_\alpha$. The eigenfunction $\tilde{Y}$ is given by the first and third components of X.

We have

$$(B(\pm\infty) + \lambda C) = \begin{pmatrix} 0 & 1 & 0 \\ \lambda + \delta & -\sigma & 0 \\ 0 & 0 & \frac{\lambda}{\sigma} \end{pmatrix}.$$

The eigenvalues are

$$\frac{\lambda}{\sigma} \quad \text{and} \quad \mu_\pm(\sigma, \delta, \lambda) = -\frac{\sigma}{2} \pm \left(\frac{\sigma^2}{4} + \lambda + \delta\right)^{\frac{1}{2}}.$$

For $\operatorname{Re}\lambda \geq \max(\omega_-, \omega_+)$, (5.4) has linear independent solutions $X^1(\xi, \lambda)$ and $X^2(\xi, \lambda)$ such that $e^{\alpha_-\xi}X^i(\xi, \lambda)$, $i = 1, 2$, is bounded for $\xi \leq 0$; they correspond to the eigenvalues $\frac{\lambda}{\sigma}$ and $\mu_+(\sigma, \delta, \lambda)$, which have real part small negative or larger. Similarly, (5.4) has, up to scalar multiplication, a unique solution $X^3(\xi, \lambda)$ such that $e^{\alpha_+\xi}X^3(\xi)$ is bounded for $\xi \geq 0$. It corresponds to the eigenvalue $\mu_-(\sigma, \delta, \lambda)$, which has a large negative real part. These solutions can be chosen to depend analytically on λ. The Evans function $D(\lambda)$ is defined for $\operatorname{Re}\lambda \geq \max(\omega_-, \omega_+) < 0$ by

$$D(\lambda) = \det\left(X^1(0, \lambda), X^2(0, \lambda), X^3(0, \lambda)\right).$$

It is analytic, and it is 0 if and only if λ is an eigenvalue of L on $\mathcal{E}_\alpha$. The algebraic multiplicity of λ as an eigenvalue of L equals its multiplicity as a zero of D.

Up to scalar multiplication, there is unique solution $\psi(\xi, \lambda)$ of the adjoint equation $\psi_\xi = -(B(\xi) + \lambda C)^\top\psi$ such that $e^{-\alpha_+\xi}\psi(\xi)$ is bounded on $\xi \leq 0$. It corresponds to the eigenvalue $-\mu_-(\sigma, \delta, \lambda)$ of $-(B(\pm\infty) + \lambda C)^\top$, which has a large positive real part. The Evans function can be equivalently defined as $D(\lambda) = \psi(0, \lambda)^\top X^3(0, \lambda)$. (More commonly, one uses $\bar{\lambda}$ instead of λ in the definition of the adjoint equation, and $\bar{\psi}(0, \lambda)^\top X^3(0, \lambda)$ in the definition of the Evans function, but the two definitions of the Evans function are equivalent.)

For the traveling wave we use linear approximations on $(-\infty, -k]$ and on $[k, \infty)$, and a numerically computed approximation on $[-k, k]$.

To approximate $D(\lambda)$, choose $-k_\ell < 0 < k_r$. Let $X(k_r) = (1, \mu_-, 0)$, which is the eigenvector of $B(\pm\infty) + \lambda C$ for the eigenvalue μ_-, and solve $X_\xi = (B(\xi) + \lambda C)X$ backward to obtain $X(0)$; let $\psi(-k_\ell) = (\lambda + \delta, \mu_-, 0)$, which is the eigenvector of $-(B(\pm\infty) + \lambda C)^\top$ for the eigenvalue $-\mu_-$, and solve $\psi_\xi = -(B(\xi) + \lambda C)^T\psi$ forward to obtain $\psi(0)$. Then $D(\lambda)$ is approximately $\psi(0)^\top X(0)$. One computes $D(\lambda)$ on an appropriate large closed curve Γ that surrounds 0. From the analyticity of D, if the winding number is 1, the only zero of the Evans function inside Γ is 0. This is numerical evidence that the only zero of the Evans function in $\operatorname{Re}\lambda \geq 0$ is 0.

A drawback of this approach is that computed values of $D(\lambda)$ have enormous modulus (because of the exponential growth of $X(\xi)$ and $\psi(\xi)$), and the curve $D(\lambda)$ can exhibit numerous twists (because of the behavior of the imaginary parts of $X(\xi)$ and $\psi(\xi)$ as they change enormously). To correct these effects, one can first define $\tilde{X}(\xi) = e^{-\mu_-(\xi - k_r)}X(\xi)$, let $\tilde{X}(k_r) = (1, \mu_-, 0)$, note that $\tilde{X}_\xi = (B(\xi) + \lambda C - \mu_- I)\tilde{X}$, and solve this equation backward to obtain $\tilde{X}(0)$. Similarly, one can define $\tilde{\psi}(\xi) = e^{\mu_-(\xi + k_\ell)}\psi(\xi)$, let $\tilde{\psi}(-k_\ell) = (\lambda + \delta, \mu_-, 0)$, note that $\tilde{\psi}_\xi = (B(\xi) + \lambda C + \mu_- I)^\top \tilde{\psi}$, and solve this equation forward to obtain $\tilde{\psi}(0)$; finally one defines $\tilde{D}(\lambda)$ to be $\tilde{\psi}(0)^\top \tilde{X}(0)$. Since $\tilde{D}(\lambda) = e^{\mu_-(k_r + k_\ell)}D(\lambda)$, the two functions have the same winding number about 0 on Γ.

We now show some computational results with $(\beta, \bar{u}_1, \kappa) = (1, 0, 0)$.

The computed curve in the $\delta\sigma$-plane for which traveling waves exist is shown in Figure 5.1.

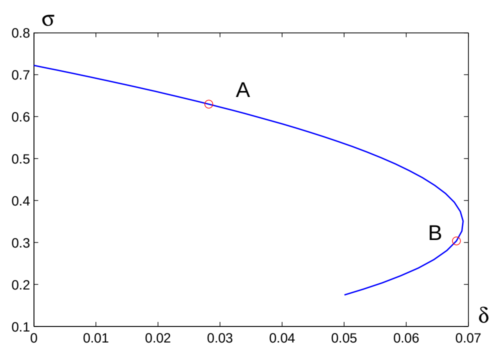

FIGURE 5.1.

For point A in Figure 5.1, we computed $\tilde{D}(\lambda)$ on several curves consisting of a right half-circle centered at $z_0 = -0.01$, together with the vertical diameter of that circle. The numbers k_ℓ and k_r were increased until the desired precision was achieved. Figures 5.2 and 5.3 show the images when the radius is 1 and 100 respectively. The winding number about 0 is 1 in both cases.

For point B in Figure 5.1, the image of the same curve with radius 1 is shown in Figure 5.4. The winding number is 2, because the Evans function has a positive real root. The new root, which causes instability of the traveling wave, crosses the imaginary axis into the right half-plane at the turning point of the curve in Figure 5.1.

REFERENCES

[1] BAYLISS, A., and MATKOWSKY, B., *Fronts, relaxation oscillations, and period doubling in solid fuel combustion*, J. Comput. Phys. **71** (1987), 147–168.

[2] BALASURIYA, S., GOTTWALD, G., HORNIBROOK, J., and LAFORTUNE, S., *High Lewis number combustion wavefronts: a perturbative Melnikov analysis*, SIAM J. Appl. Math. **67** (2006–07), 464–486

[3] BERESTYCKI, H., NICOLAENKO, B., and SCHEURER, B., *Traveling wave solutions to combustion models and their singular limits*, SIAM J. Math. Anal. **16** (1985), 1207–1242.

[4] BILLINGHAM, J., *Phase plane analysis of one-dimensional reaction diffusion waves with degenerate reaction terms*, Dyn. Stab. Syst. **15** (2000), 23–33.

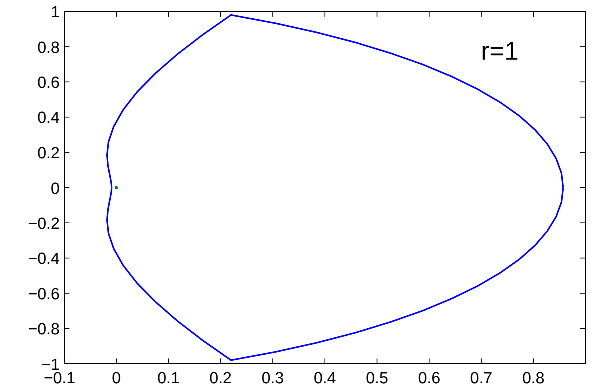

Figure 5.2.

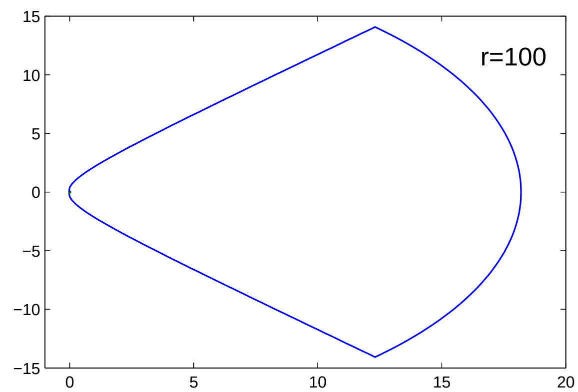

Figure 5.3.

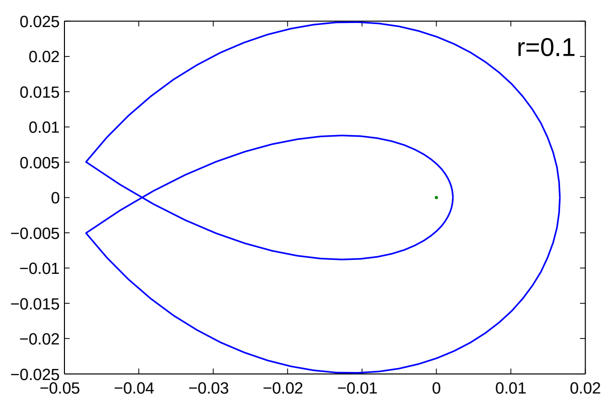

Figure 5.4.

[5] Giovangigli, V., *Nonadiabatic plane laminar flames and their singular limits*, SIAM J. Math. Anal. **21** (1990), 1305–1325.

[6] Ghazaryan, A., *Nonlinear stability of high Lewis number combustion fronts*, Indiana Univ. Math. J. **58** (2009), 181–212.

[7] Ghazaryan, A., and Jones, C. K. R. T., *On the stability of high Lewis number combustion fronts*, Discrete Contin. Dyn. Syst. **24** (2009), 809–826.

[8] Ghazaryan, A., Latushkin, Y., Schecter, S., and de Souza, A. J., *Stability of gasless combustion fronts in one-dimensional solids*, Arch. Ration. Mech. Anal. **198** (2010), 981–1030.

[9] Ghazaryan, A., Latushkin, Y., and Schecter, S., *Stability of traveling waves for degenerate systems of reaction diffusion equations*, to appear in Indiana Univ. Math. J..

[10] Ghazaryan, A., Latushkin, Y., and Schecter, S., *Stability of traveling waves for a class of reaction-diffusion systems that arise in chemical reaction models*, SIAM J. Math. Anal. **42** (2010), 2434–2472.

[11] Gubernov, V. V., Mercer, G. N., Sidhu, H. S., and Weber, R. O., *Evans function stability of combustion waves*, SIAM J. Appl. Math. **63** (2003), 1259–1275.

[12] Gubernov, V. V., Sidhu, H. S., and Mercer, G. N., *The effect of ambient temperature on the propagation of nonadiabatic combustion waves*, J. Math. Chem. **37** (2005), 149–162.

[13] Kato, T., *Perturbation theory for linear operators*, second edition, Grundlehren der Mathematischen Wissenschaften, Band 132, Springer-Verlag, Berlin-New York, 1976.

[14] Logak, E., *Mathematical analysis of a condensed phase combustion model without ignition temperature*, Nonlinear Anal. **28** (1997), 1–38.

[15] Logak, E., and Loubeau, V., *Travelling wave solutions to a condensed phase combustion model*, Asymptotic Anal. **12** (1996), 259–294.

[16] Marion, M., *Qualitative properties of a nonlinear system for laminar flames without ignition temperature*, Nonlinear Anal. **9** (1985), 1269–1292.

[17] Roques, L., *Study of the premixed flame model with heat losses: The existence of two solutions*, European J. Appl. Math. **16** (2005), 741765.

[18] Sandstede, B., *Stability of travelling waves*, in Handbook of Dynamical Systems, Vol. 2, 983–1055, North-Holland, Amsterdam, 2002.

[19] Schecter, S., *The saddle-node separatrix-loop bifurcation*, SIAM J. Math. Anal. **18** (1987), 1142–1156.

[20] Simon, P., Merkin, J., and Scott, S., *Bifurcations in non-adiabatic flame propagation models*, Focus on Combustion Research (2006), 315–357.

[21] Varas, F. and Vega, J., *Linear stability of a plane front in solid combustion at large heat of reaction*, SIAM J. Appl. Math. **62** (2002), 1810–1822.

Department of Mathematics, Miami University, Oxford, Ohio 45056, USA, +1-513-529-0582
E-mail address: ghazarar@muohio.edu

Department of Mathematics, North Carolina State University, Box 8205, Raleigh, North Carolina 27695, USA, +1-919-515-6533
E-mail address: schecter@ncsu.edu

Department of Applied Analysis and Computational Mathematics, Eötvös Loránd University, Budapest, Hungary, +36-1-272-2500
E-mail address: simonp@cs.elte.hu